HHS Public Access

Author manuscript

Cell Immunol. Author manuscript; available in PMC 2024 April 16.

Published in final edited form as:

Cell Immunol. 2023 April ; 386: 104690. doi:10.1016/j.cellimm.2023.104690.

Downregulation of a tumor suppressor gene LKB1 in lung transplantation as a biomarker for chronic murine lung allograft rejection

Mohammad Rahman[a,§], **Ranjithkumar Ravichandran**[a,$], **Narendra V. Sankpal**[a], **Sandhya Bansal**[a], **Angara Sureshbabu**[a], **Timothy Fleming**[a], **Sudhir Perincheri**[b], **Ankit Bharat**[c], **Michael A. Smith**[a], **Ross M. Bremner**[a], **T. Mohanakumar**[a,*]

[a]Norton Thoracic Institute, St. Joseph's Hospital and Medical Center, Phoenix, AZ 85013

[b]Yale University School of Medicine, West Haven, CT

[c]Northwestern University, Chicago, Illinois

Abstract

Background: We recently demonstrated decreased tumor suppressor gene liver kinase B1 (LKB1) level in lung transplant recipients diagnosed with bronchiolitis obliterans syndrome. STE20-related adaptor alpha (STRADα) functions as a pseudokinase that binds and regulates LKB1 activity.

Methods: A murine model of chronic lung allograft rejection in which a single lung from a B6D2F1 mouse was orthotopically transplanted into a DBA/2J mouse was employed. We examined the effect of LKB1 knockdown using CRISPR-CAS9 *in vitro* culture system.

Results: Significant downregulation of LKB1 and STRADα expression was found in donor lung compared to recipient lung. STRADα knockdown significantly inhibited LKB1, pAMPK expression but induced phosphorylated mammalian target of rapamycin (mTOR), fibronectin, and Collagen-I, expression in BEAS-2B cells. LKB1 overexpression decreased fibronectin, Collagen-I, and phosphorylated mTOR expression in A549 cells.

[*]**Corresponding Author:** T. Mohanakumar, Ph.D., Norton Thoracic Institute, 124 W Thomas Road, Suite 105, Phoenix, AZ 85013, tm.kumar@dignityhealth.org, Phone: 602-406-8347.

[§]Authors have equal contributions.

Credit authorship contribution statement

Conceptualization: T. Mohanakumar, M Rahman

Methodology: M Rahman, N Sankpal, S Bansal

Writing/editing: M Rahman, T Mohanakumar, S Angara, T Fleming,

Editing: R Bremner, M Smith, A Bharat

Analysis: M Rahman, R Ravichandran, S Perincheri

Declaration of competing interest

The authors declare that they have no known competing financial interests or personal relationships that could have appeared to influence the work reported in this paper.

Conclusions: We demonstrated that downregulation of LKB1-STRADα pathway accompanied with increased fibrosis, results in development of chronic rejection following murine lung transplantation.

1. INTRODUCTION

Lung transplantation (LTx) is the only life-extending option for patients with end-stage lung diseases. Approximately half of LTx recipients (LTxRs) clinically diagnosed with chronic lung allograft dysfunction (CLAD) will experience chronic rejection within 5 years of transplant [1]. CLAD is defined as a substantial and persistent decline (≥20%) in measured forced expiratory volume in 1 second (FEV_1) value from the reference (baseline) value. The baseline value is computed as the mean of the best 2 post-operative FEV_1 measurements (taken >3 weeks apart) [2]. The prevalence of bronchiolitis obliterans syndrome (BOS), a condition in which the bronchioles become inflamed and fibrotic, a subtype of CLAD. The incidence ranges from 30–40% within 5 years, and BOS is the most significant cause of long-term graft failure and mortality after LTx [3]. CLAD results primarily from immunological insults to transplanted lungs. Significant correlations between BOS and post-transplant development of antibodies to mismatched donor human leukocyte antigens (HLAs), that is, donor-specific antibodies and antibodies to the lung self-antigens (SAgs), K-alpha 1 tubulin and Collagen V (Col-V), have been reported [4, 5].

Recent studies have shown that exosomes play an important role in gene expression [6], cellular signaling [7], epithelial mesenchymal transition [8], and disease progression [9]. Three types of extracellular vesicles have been classified according to their diameter: exosomes (30–200 nm), microvesicles (200–500 nm), and apoptotic bodies (500–1000 nm) [10]. Recently, our laboratory has demonstrated that exosomes isolated from BOS inhibit tumor suppressor gene liver kinase B1 (LKB1) expression and induce epithelial mesenchymal transition (EMT) in both HPBEC and BEAS-2B cells [11]. It has been shown that EMT plays an important role in airway remodeling [12] and Borthwick and colleagues [13] have demonstrated that EMT may underlie the dysfunctional airway repair processes that lead to obliterans bronchiolitis.

At present, the mechanism by which LKB1 affects BOS development is unknown, and therapeutic options to prevent or treat BOS are unavailable. It has also been reported that disruption of cellular polarity may induce fibrosis, a hallmark of CLAD [14, 15]. LKB1 is required to maintain cell polarity and control growth through protease-activated receptor-1 and AMP-activated protein kinase (AMPK), respectively [16, 17]. LKB1 plays a critical role in EMT [18], differentiation [19], migration [20], and mammalian target of rapamycin (mTOR) signaling [21]. EMT (or EMT-like processes) may affect the development of BOS after human LTx. Furthermore, increased phosphorylation of mTOR is closely associated with pulmonary fibrosis [22]. LKB1 signaling controls energy metabolism [23] and tissue homeostasis [24], and deletion of the LKB1 gene is embryonic-lethal [25]. Germline mutations in LKB1 are associated with a predisposition to Peutz-Jeghers syndrome [26], an inherited condition that increases cancer risk. Loss of LKB1 expression by either somatic mutations or promoter hypermethylation is frequently identified in several cancer types including lung cancer [27]. The role of LKB1 and its downstream regulators and the link to

AMPK signals in the development of BOS after LTx have not been studied. STE20-related adaptor alpha (STRADα) functions as a pseudokinase that consists of an STE20-like kinase domain but lacks several residues required for intrinsic catalysis [28, 29]. STRADα is an essential co-factor for LKB1-mediated G1-phase cell cycle arrest [30, 31]. We examined the effect of STRADα on LKB1 expression.

In this study using a murine model of chronic lung allograft rejection (B6D2F1 to DBA/2J) [32], we demonstrated that the downregulation of the LKB1-STRADα axis modulated AMPK and mTOR phosphorylation which increase fibrosis of transplanted lung.

2. METHODS

2.1 Animals and orthotopic LTx model

A murine model of chronic lung allograft rejection was established as described by Mimura et al [32]. In brief, a single lung from a B6D2F1 (H2b/d) donor mouse was orthotopically transplanted into a DBA/2 (H2d) recipient (10–12 weeks old) weighing 28–30 g. Specific pathogen-free male inbred mice B6D2F1/J (H2b/d) and DBA/2J (H2d) were purchased from Jackson Laboratories (Bar Harbor, Maine, USA). All experiments were performed according to the protocols approved by the Institutional Review Board of St. Joseph's Hospital and Medical Center. In our study, >80% of the animals developed histological features of chronic lung allograft rejection of the transplanted lung by post-transplant day 34. Serum samples were collected on days 7, 14, and 34. Orthotopic left LTx was performed as previously described [32]. A surgical microscope (AmScope SM-4B-80S Professional Binocular Stereo Zoom Microscope, WH10x Eyepieces; United Scope, LLC, Irvine, California, USA) with WF10×/20× magnification was used for all procedures. Buprenorphine was administered to recipient mice at the conclusion of the procedure and every 12 h until post-transplantation day 3. No immunosuppressive drugs were administered to the patient.

2.2 Histopathologic evaluation of orthotopic LTx

Mice (n=5) were euthanized under anesthesia 34 days after transplantation. Lung blocks were fixed in 10% formalin and embedded in paraffin. The cut sections were stained with hematoxylin and eosin or Masson's trichrome to determine the presence of fibrosis. Grading for rejection was performed by blinded reviewers using the standard criteria developed by the lung rejection study group.

2.3 Immunohistochemistry of mouse lung tissue

Mouse lung tissue was fixed in neutralized 10% formalin and embedded in paraffin blocks, which were cut into 4–5 mm thick sections and mounted on slides (Leica Biosystems, Buffalo Grove, Illinois, USA) for immunohistochemistry. The sections were stained with antibodies specific to LKB1 (Cell Signaling Technology, Danvers, Massachusetts, USA). Images were obtained using an Aperio microscope (Leica Biosystems) at 40× magnification, and morphometric analysis was performed using the MYNTRA software. The analysis was performed by looking at five different areas on the same slide.

2.4 Morphometric analysis for fibrosis

For evaluation of fibrosis, whole slide images of lung sections stained with trichrome stain were exported as TIFF files. Color deconvolution of the TIFF files was performed in ImageJ using a color deconvolution plugin (https://imagej.net/Colour_Deconvolution). The extent of blue-staining collagenous fibrosis was then determined using standard tools available in the ImageJ suite.

2.5 Exosome isolation and characterization

We characterized the exosomes isolated from mouse serum as previously described [11]. In brief, circulating exosomes were isolated from serum collected from mouse LTxRs using the Total Exosome Isolation Kit (Invitrogen, Thermo Fisher Scientific, Waltham, Massachusetts, USA) according to the manufacturer's protocol. The serum was centrifuged at 10,000 g for 20 min to remove debris, diluted with phosphate-buffered saline PBS (0.5 volume) and exosome precipitation solution (0.2 volume), incubated for 10 min, and centrifuged at 10,000 × g for 5 min at room temperature. The exosome pellet was dissolved in PBS and used for all the analyses. Exosome size distribution was measured using a NanoSight (Malvern Panalytical Ltd, Malvern, UK), and 30–200 nm diameter particles were classified as exosomes.

2.6 Western blot analysis

Western blotting was performed on total protein extracts from exosomes and mouse lung tissues. RIPA lysis buffer with protease and phosphatase inhibitor cocktails (Sigma-Aldrich, St. Louis, Missouri, USA) was used to determine the total protein fraction. Protein concentrations in the cell extracts and exosomes were determined using a bicinchoninic acid protein assay (Thermo Fisher Scientific) to standardize for quantification. Twenty micrograms of total lysates were diluted 1:1 in RIPA SDS-PAGE sample buffer, loaded onto polyacrylamide gels, and blotted onto PVDF membranes (Bio-Rad, Hercules, California, USA). Membranes were blocked with 5% non-fat milk in PBS (pH 7.6) and 0.2% Tween-20 for 1 h and then incubated overnight with primary antibodies: mouse monoclonal anti-CD63 (1:1000, Santa Cruz Biotechnology), rabbit polyclonal anti-LKB1 (1:1000, Cell Signaling Technology), rabbit polyclonal anti-AMPK (1:1000, Cell Signaling Technology), rabbit polyclonal anti-phosphorylated AMPK (Thr 172) (pAMPK; 1:1000, Cell Signaling Technology), mouse monoclonal anti-phosphorylated mTOR (Ser 2448) (1:500, Santa Cruz Biotechnology), mouse monoclonal anti-mTOR (1:500, Santa Cruz Biotechnology), mouse monoclonal anti-STRADα (1:1000, Santa Cruz), mouse monoclonal anti-fibronectin (FN) (1:1000, Santa Cruz Biotechnology, Santa Cruz, California, USA), and rabbit polyclonal anti-Col-I (1:1000, Abcam plc, Cambridge, UK). After washing in PBS Tween-20, the membranes were incubated with horseradish peroxidase-conjugated goat anti-rabbit (1:2000, Cell Signaling Technology) or anti-mouse antibodies (1:2000, Cell Signaling Technology), and the immunoblots were visualized using ECL detection kits (Pierce, Rockford, Illinois, USA). Mouse anti-GAPDH antibody (1:5000) was used as the internal control.

2.7 BEAS-2B cell culture and STRADα knockdown by siRNA

BEAS-2B cells, an immortalized human bronchial epithelial cell line, were purchased from the American Type Culture Collection (Manassas, Virginia, USA). BEAS-2B cells were grown in RPMI-1640 complete medium containing 10% fetal bovine serum and 100 U/mL penicillin-streptomycin. The cells were maintained in a 10 cm petri dish in a 5% CO2 and 37°C humidified environment. Cells from passages 2–7 were used throughout the experiments at an initial seeding density of $6–7\times10^4$ cells/cm^2 unless otherwise mentioned. For siRNA delivery (STRADα; Santa Cruz Biotechnology), 1×10^5 cells were grown in a 6-well plate for 24 h in antibiotic-free medium, and 80 pmol of siRNA were transfected using Lipofectamine™ 2000 (Invitrogen, Thermo Fisher Scientific).

2.8 BEAS-2B cell culture and knockdown of LKB1

A BEAS-2B LKB1 knockdown cell line was generated with previously validated LKB1 gRNA [33]. To generate a stable knockdown, LentiCRISPRv2-sgLKB1 clone1 or clone2 (Addgene, Watertown, MA, USA# 162125 and #162126) were transiently transfected together with lentiCas9-Blast (Addgene #52962) using FugeneHD. After 2 days, the cells were selected with blasticidin (5μg/mL) and puromycin (2μg/mL) for a week. LKB1 gene silencing was verified by western blotting. sgLKB1-clone2 showed 100% LKB1 ablation and was used throughout the study.

2.9 A549 cell culture and overexpression of LKB1

Generation of LKB1 expressing stable lines: —Retro-viral vectors, pBABE or Pbabe-LKB1 were obtained from Addgene (Cambridge, MA). A549 cells were transfected with viral plasmids using Lipofactamine-LTX. Retroviral particles were harvested from media supernatants after 48 h. PBabe or pBabe-LKB1 virus media was filtered through 0.45 micron filters and added to A549 cells with polybrene (10 ug/mL) overnight. After two subsequent transductions, A549 cells were selected with 2 μg/ml puromycin for 1 week before performing experiments.

2.10 LKB1 signaling pathway analysis

We used MEK inhibitor (trametinib, 1μM), JNK inhibitor (SP600125, 10 μM), P38 mitogen-activated protein kinase (MAPK) inhibitor (SB203580, 10 μM), PI3K inhibitor (LY294002, 10 μM), mTOR inhibitor (rapamycin, 1 μM), AMPK inhibitor (AICAR, 500 μM), ROCK inhibitor (Y-27632, 10 μM) and proteasome inhibitor (bortezomib, 0.1 μM) to screen the LKB1-mediated signaling pathways. Both wild-type and LKB1 knockdown BEAS-2B cell lines were treated with the above-mentioned inhibitors at different concentrations for 12 h. The cells were then washed with PBS and treated with inhibitors for 1 h. Finally, 20% fetal bovine serum was added for 2 h, and the protein was harvested.

2.11 Statistical analysis

Statistical analysis was calculated with GraphPad Prism 6 (GraphPad Software Inc, La Jolla, Calif). Statistical data was expressed as mean ± standard deviation. P values less than 0.05 were considered statistically significant in each analysis. ImageJ software was used to quantify optical density of blot. Fold changes are based on experiment versus control of each

group. We used one way ANOVA followed by Tukeys t-test 2-tailed nonparametric to detect statistical significance.

3. RESULTS

3.1 NanoSight tracking analysis (NTA) demonstrates that isolated vesicles were exosomes (40~200nm)

NTA and Western blot were used to characterize the size and estimated number/ml of isolated nanoparticles from mouse serum. We measured the average size distribution of nanoparticles isolated from mouse serum using our isolation technique (Figure 1A). The curves demonstrate that the average number of nanoparticles/ml measured using the NTA system was 5.4×10^6 from mouse serum) (Data was compiled from five measurements per biological replicates (n=3). Particles used in this report had a size of <200 nm and were considered exosomes, in agreement with the recommendation made by the nomenclature committee on exosomes [34]. According to the committee we also characterized the exosomes by Western blot. CD63, TSG-101, and Alix were used as exosome marker and Calnexin was used as cell marker (Figure 1B).

3.2 Increased levels of circulating exosomes by days 14 and 34 after murine LTx

The number of exosomes released into circulation was significantly higher in the transplanted mice on day 14 (3333333±88196.71; p=0.04) and day 34 (3501000±131343.06; p=0.02) than in control mice (2265000±90737.72; Figure 1C).

3.3 LKB1 expression is downregulated in circulating exosomes as well as in the donor lung tissue in transplanted mice

To investigate the expression of LKB1 in circulating exosomes, we first characterized the total number of exosomes present in transplanted (n=5) and non-transplanted DBA/2 mice (n=5). Blood was collected from mice on days 7, 14, and 34. Exosomes were purified and characterized using NanoSight, as described in Methods. Forty micrograms of protein isolated from each transplanted (n=5) and non-transplanted (n=5) mouse on days 7, 14, and 34 were analyzed by western blotting. The purity of exosomes was confirmed using CD63 as an exosome marker and GAPDH as a loading control. Densitometric analysis of the bands showed that LKB1 levels were significantly lower on day 34 (p=0.02), about 2–3 fold in the transplanted mice than in the control mice (Figure 2A, 2B). We also determined the expression of LKB1 in donor lung tissue at day 34 by immunohistochemistry. We also found downregulation of LKB1 in donor lung tissue compared to recipient lung (Figure 2C).

3.4 LKB1, STRADα, and pAMPK were downregulated, but phosphorylated mTOR was upregulated in donor lungs

Exosomes derived from transplanted mice with chronic rejection showed lower LKB1 expression (Figure 2A, 2B). Thus, we anticipated the impact of AMPK phosphorylation on LKB1 expression. Immunohistochemistry on day 34 after transplantation showed that LKB1 was downregulated in the donor lung tissue compared to that in the recipient native lung tissue (Figure 2C). Furthermore, western blot analysis confirmed the downregulation of LKB1 together with its binding partner STRADα and downstream substrate phosphorylated

AMPK (pAMPK) in donor lung tissue compared to recipient native lung tissue. Surprisingly, phosphorylated mTOR (pmTOR) levels were significantly higher in the donor lung than in the recipient lung (Figure 3A). Quantitative densitometry analysis showed significantly lower levels of STRADα (p=0.002), LKB1 (p=0.013), and pAMPK Thr 172 (p=0.01) but significantly higher levels of pmTOR Ser2448 (p=0.006) in donor lungs than in recipient native lungs (Figures 3B, C, D, E). These results indicate that LKB1 and STRADα expression is dysregulated in transplanted lungs.

3.5 Histological evidence of chronic rejection in the transplanted but not native lung

To assess chronic rejection, we first analyzed donor (n=5) and native (n=5) lung samples from the DBA/2 orthotopic LTx mice. Specimens were collected 34 days after transplantation. The cut sections were stained with Masson's trichrome to determine the presence of fibrotic lesions. Donor lungs in the B6D2F1/J to DBA/2J orthotopic LTx model developed significantly more fibrosis than recipient native lungs, indicative of chronic rejection (Figure 4A, B). Quantitation analysis revealed that approximately 82% of the tissue area of the transplanted lung demonstrated fibrosis associated with chronic inflammation; however, only 18% of the tissue in the native lung had these features (Figure 4C). Together, these results demonstrate that the B6D2F1/J to DBA/2J orthotopic LTx murine model induces fibrosis and chronic rejection of the transplanted lung.

3.6 Extracellular matrix markers FN and Col-I are Upregulated in the Donor Lung

Fibrosis is often characterized by the presence of FN and Col-I. Since extracellular matrix dynamics are altered during tissue injury, we analyzed the expression of the major components of the matrix (FN and Col-I) by western blotting. As expected, the expression of both FN and Col-I were significantly higher in donor lungs than in recipient native lungs (Figure 5A). Densitometry confirmed significant upregulation of FN (Figure 5B; p=0.04) and Col-I (Figure 5C; p=0.001) in donor lungs compared to recipient lungs. Altogether, donor lung samples and circulating exosomes showed higher expression of extracellular matrix markers and lower expression of LKB1 and STRADα.

3.7 STRADα knockdown with siRNA significantly inhibited LKB1 and pAMPK and induced pmTOR expression in BEAS-2B cells

LKB1–STRADα-MO25 protein complex formation is necessary for LKB1 kinase activity as an active conformation for signaling [35]. To recreate STRADα loss similar to that seen after LTx (Figures 3A), STRADα knockdown cells were generated. After efficient transfection of BEAS-2B cells with STRADα siRNA, cells were subjected to western blot analysis. Our data demonstrated that STRADα-knockdown cells exhibited lower levels of LKB1 and its downstream substrate/kinase pAMPK Thr 172 while no change in total AMPK was observed. Higher levels of phosphorylated mTOR Ser 2448 were also observed in STRADα-knockdown BEAS-2B cells than in control cells or cells transfected with non-targeting siRNA (Figure 6A). Quantitative densitometry analysis showed significantly higher levels of STRADα (Figure 6B; p=0.004), LKB1 (Figure 6C; p=0.004), and pAMPK (Figure 6D; p=0.003) and significantly lower levels of phosphorylated mTOR Ser2448 (Figure 6E; p=0.018). These results demonstrate that STRADα knockdown dysregulates AMPK and mTOR phosphorylation in an LKB1-dependent manner.

3.8 STRADα knockdown upregulated FN and Col-I in BEAS-2B cells

Figure 5 data shows that exosomes isolated from serum after LTx have higher levels of extracellular matrix markers. We anticipated that ablation of STRADα from the LKB1–STRADα complex may have a similar effect. Western blot analysis showed that BEAS-2B cells subjected to STRADα knockdown had higher levels of both FN and Col-I than controls (Figure 7A). Densitometric analysis showed that compared to control siRNA knockdown, STRADα siRNA knockdown significantly upregulated FN ($p=0.001$; Figure 7B) and Col-I ($p=0.008$; Figure 7C). These results suggest STRADα plays an important role in the development of fibrosis.

3.9 mTOR inhibition decreased FN and Col-1 expression in control and LKB1 knockout BEAS-2B cells

Since the loss of LKB1 and STRADα mimicked similar results, regulating the loss of LKB1 and the gain of extracellular matrix markers as an indication of fibrosis progression, we aimed to identify a major signaling pathway involved in this process. To this end, we used inhibitors of MEK, JNK, P38MAPK, PI3K, mTOR, AMPK, ROCK, and proteasome. We generated a CRISPR-CAS9–mediated LKB1 knockdown stable BEAS-2B cell line with previously characterized gRNA. Among all inhibitors, we observed that the extracellular matrix marker FN increased only when mTOR phosphorylation increased. Furthermore, only the mTOR inhibitor rapamycin (1 μM) significantly downregulated FN and Col-I expression (Figure 8A, B, C).

3.10 LKB1 overexpression downregulates FN, Col-I, and phosphorylated mTOR in A549 cells

We have shown LKB1 downregulation induces FN, Col-I, and phosphorylated mTOR. To check the effect, either LKB1 dependent or not, we overexpressed LKB1 in A549 cells and examined the expression of FN, Col-I, and phosphorylated mTOR. We found LKB1 overexpression in A549 cells downregulated the expression of FN, Col-I, and phosphorylated mTOR (Figure 8D), suggests that LKB1 play direct role on FN, Col-I, and phosphorylated mTOR in A549 cells.

3.11 Schematic diagram of LKB1 deficiency in the development of fibrosis in the lung

LKB1 downregulation inhibits AMPK phosphorylation which, in turn, induces upregulation of mTOR phosphorylation and EMT. Both EMT and mTOR phosphorylation induces fibrosis in the lung.

4. DISCUSSION

Circulating exosomes and their contents have been shown to play an important role in the pathogenesis of human diseases including cancer and infections as well as cardio metabolic and neurological health [36–39]. Our previous studies demonstrated higher levels of circulating exosomes with lung SAgs and donor HLA in LTxRs undergoing rejection, suggesting that the exosomes originated from the transplanted lungs [40]. We also reported that circulating exosomes with lung SAgs can be detected 12 months before the clinical diagnosis of chronic lung allograft rejection, suggesting that circulating exosomes with lung

SAgs can be a noninvasive biomarker for identifying LTxRs at risk for chronic rejection [41]. BOS lesions are often patchy and biopsy results are not very reliable. Due to this problem, ISHLT defined BOS mostly using clinical criterion [42]. Therefore, we propose that LKB1 level of exosomes should be more reliable and noninvasive compared to the use of lung biopsy samples. Recently, we demonstrated increased exosomes in circulation during BOS after human LTx [11]. In the current study, using a murine model of chronic rejection, NanoSight tracking indicated higher levels of circulating exosomes (30–200 nm in diameter) in the transplanted mice undergoing rejection than in control mice, corroborating our findings in human LTxRs. However, the mechanism by which these exosomes increase in mice and humans before and during chronic rejection remains unknown. The results presented here strongly suggest that downregulation of STRADα leads to the loss of LKB1 expression, which increases the expression of fibrotic markers, Col-I and FN, in human bronchial epithelial cells. Overexpression of LKB1 in A549 cells (LKB1 is inactivated), decreased the expression of FN, Col-I, and phosphorylated mTOR expression compared to control. These results strongly suggests that LKB1 has a direct role on fibrosis development. LKB1 has several functions in nutrient sensing, including in p53-related pathways [17] and Rab7 interactions [43]. Currently, it is unclear which pathways downstream of LKB1 are critical for exosome release.

We recently demonstrated that, compared to exosomes isolated from stable LTxRs, circulating exosomes isolated from LTxRs with BOS contained lower levels of LKB1 expression at both the mRNA and protein levels [11]. In the current study, employing a murine model of chronic lung allograft rejection, we also demonstrate that circulating exosomal proteins derived from transplanted mice undergoing chronic rejection had lower levels of LKB1. Furthermore, LKB1 was significantly downregulated in transplanted donor lungs compared to that in recipient native lungs. Further, STRADα, an upstream regulator of LKB1, plays a role in the downregulation of LKB1 in both exosomes and transplanted lungs. However, it is unclear whether the downregulation of STRADα initially occurs in the transplanted lung or in circulating exosomes. Recently, it has been reported that STRADα is part of the STE-20-like kinase family, which stimulates MAPK pathways by activating MAPK kinase kinase [30]. The protein forms a heterotrimeric complex with LKB1, and this complex can bind to calcium-binding protein 39 (CAB39, also known as MO25) [30]. STRADα is an upstream activator of LKB1 and also leads to the subcellular localization of LKB1 by fixing it in the cytoplasm [30]. The interaction between STRADα and LKB1 leads to the phosphorylation of STRADα and enhanced autophosphorylation of LKB1 [30]. The protein activates LKB1 leading to the phosphorylation of both proteins and excluding LKB1 from the nucleus [30]. Another novel finding in this study is that STRADα was downregulated in the transplanted donor lungs but not in the recipient native lungs. We found that knockdown of STRADα by siRNA significantly inhibited LKB1 and AMPK phosphorylation in BEAS-2B cells. These results demonstrate that STRADα plays an important role in the downregulation of LKB1 in the transplanted lung.

Increased inflammation after transplantation and activation of immune pathways, including the development of antibodies to donor HLAs and/or lung SAgs, may contribute to the downregulation of STRADα leading to the downregulation of LKB1. Another possibility is that immune activation directly contributes to the downregulation of both STRADα

and the tumor suppressor gene LKB1. The downregulation of LKB1 can induce EMT in transplanted lungs, contributing to the pathogenesis of BOS. We recently demonstrated that downregulation of LKB1 induced EMT markers in human alveolar epithelial cells and that knockdown of LKB1 by siRNA induced the production of vimentin and α-SMA in BEAS-2B cells [11]. In our pathway inhibitor analysis (Figure 8), we found the loss of LKB1 increased mTOR activation, and treating these cells with mTOR inhibitor significantly decreased FN and Col-I expression. This is in agreement with a recent report demonstrating that mTOR inhibition significantly suppressed TGF-β induced FN and Col-I expression in human trabecular meshwork cells [44]. Recently, it has been reported that autophagy and LKB1 work synergistically to maintain adult mouse homeostasis and survival [24]. Another study showed autophagy is promoted by AMPK. On the other hand, autophagy is inhibited by mTOR [45]. It has also been reported that autophagy was involved in the cold ischemia/reperfusion injury in the LTx model, and played a potential role on the regulation of ischemia/reperfusion injury after LTx [46]. We are currently investigating the correlation between LKB1 and autophagy in BOS after LTx. Based on our current findings, we hypothesize that downregulation of LKB1 inhibits phosphorylation of AMPK and increased phosphorylation of mTOR inducing fibrosis in lung after LTx.

This study had some potential limitations. First, we used a human airway epithelial cell line, BEAS-2B, to determine the mechanisms underlying LKB1 downregulation and its consequences. However, we believe that the results obtained using this cell line are relevant to the pathogenesis of BOS following human LTx. Second, our finding that STRADα is involved in the pathogenesis of BOS was only tested in the BOS subtype of CLAD, but not in the other well-recognized phenotype of CLAD, restrictive allograft syndrome.

In summary, we demonstrated an increased exosome release after orthotopic LTx in mice before and during chronic rejection. This finding supports our previous publication showing higher levels of circulating exosomes in LTxRs diagnosed with BOS than in stable LTxRs [11]. We also found that LKB1 expression is downregulated in donor lungs compared to recipient native lungs in this mouse model of chronic lung allograft rejection suggesting that LKB1 plays an important role in BOS pathogenesis. The current study also demonstrates that STRADα acts as an upstream regulator of LKB1 expression. Taken together, these results demonstrate that STRADα regulates LKB1 expression, and the downregulation of LKB1 leads to fibrosis by regulating FN and Col-I expression, therefore determining the circulating exosomal LKB1 levels could serve as a potential biomarker for LTxRs at risk for the development of BOS.

Acknowledgements

We thank Dr. Wei Liu, Microsurgery Core, for performing murine lung transplantation and Kristine Nally and Billie Glasscock for assistance with editing and manuscript preparation.

Funding Information

This work was supported by NIH HL156891(TM).

Data availability

Data will be made available upon request.

REFERENCES

[1]. Yusen RD, Edwards LB, Kucheryavaya AY, Benden C, Dipchand AI, Dobbels F, Goldfarb SB, Levvey BJ, Lund LH, Meiser B, Stehlik J, H. International Society for T. Lung, The registry of the International Society for Heart and Lung Transplantation: thirty-first adult lung and heart-lung transplant report--2014; focus theme: retransplantation, J Heart Lung Transplant, 33 (2014) 1009–1024. [PubMed: 25242125]

[2]. Verleden GM, Glanville AR, Lease ED, Fisher AJ, Calabrese F, Corris PA, Ensor CR, Gottlieb J, Hachem RR, Lama V, Martinu T, Neil DAH, Singer LG, Snell G, Vos R, Chronic lung allograft dysfunction: Definition, diagnostic criteria, and approaches to treatment-A consensus report from the Pulmonary Council of the ISHLT, J Heart Lung Transplant, 38 (2019) 493–503. [PubMed: 30962148]

[3]. Valentine VG, Robbins RC, Berry GJ, Patel HR, Reichenspurner H, Reitz BA, Theodore J, Actuarial survival of heart-lung and bilateral sequential lung transplant recipients with obliterative bronchiolitis, J Heart Lung Transplant, 15 (1996) 371–383. [PubMed: 8732596]

[4]. Safavi S, Robinson DR, Soresi S, Carby M, Smith JD, De novo donor HLA-specific antibodies predict development of bronchiolitis obliterans syndrome after lung transplantation, J Heart Lung Transplant, 33 (2014) 1273–1281. [PubMed: 25130554]

[5]. Hachem RR, Tiriveedhi V, Patterson GA, Aloush A, Trulock EP, Mohanakumar T, Antibodies to K-alpha 1 tubulin and collagen V are associated with chronic rejection after lung transplantation, Am J Transplant, 12 (2012) 2164–2171. [PubMed: 22568593]

[6]. Lloret-Llinares M, Karadoulama E, Chen Y, Wojenski LA, Villafano GJ, Bornholdt J, Andersson R, Core L, Sandelin A, Jensen TH, The RNA exosome contributes to gene expression regulation during stem cell differentiation, Nucleic Acids Res, 46 (2018) 11502–11513. [PubMed: 30212902]

[7]. Corrado C, Raimondo S, Chiesi A, Ciccia F, De Leo G, Alessandro R, Exosomes as intercellular signaling organelles involved in health and disease: basic science and clinical applications, Int J Mol Sci, 14 (2013) 5338–5366. [PubMed: 23466882]

[8]. Rahman MA, Barger JF, Lovat F, Gao M, Otterson GA, Nana-Sinkam P, Lung cancer exosomes as drivers of epithelial mesenchymal transition, Oncotarget, 7 (2016) 54852–54866. [PubMed: 27363026]

[9]. Gunasekaran M, Bansal S, Ravichandran R, Sharma M, Perincheri S, Rodriguez F, Hachem R, Fisher CE, Limaye AP, Omar A, Smith MA, Bremner RM, Mohanakumar T, Respiratory viral infection in lung transplantation induces exosomes that trigger chronic rejection, J Heart Lung Transplant, 39 (2020) 379–388. [PubMed: 32033844]

[10]. Yanez-Mo M, Siljander PR, Andreu Z, Zavec AB, Borras FE, Buzas EI, Buzas K, Casal E, Cappello F, Carvalho J, Colas E, Cordeiro-da Silva A, Fais S, Falcon-Perez JM, Ghobrial IM, Giebel B, Gimona M, Graner M, Gursel I, Gursel M, Heegaard NH, Hendrix A, Kierulf P, Kokubun K, Kosanovic M, Kralj-Iglic V, Kramer-Albers EM, Laitinen S, Lasser C, Lener T, Ligeti E, Line A, Lipps G, Llorente A, Lotvall J, Mancek-Keber M, Marcilla A, Mittelbrunn M, Nazarenko I, Nolte-'t Hoen EN, Nyman TA, O'Driscoll L, Olivan M, Oliveira C, Pallinger E, Del Portillo HA, Reventos J, Rigau M, Rohde E, Sammar M, Sanchez-Madrid F, Santarem N, Schallmoser K, Ostenfeld MS, Stoorvogel W, Stukelj R, Van der Grein SG, Vasconcelos MH, Wauben MH, De Wever O, Biological properties of extracellular vesicles and their physiological functions, J Extracell Vesicles, 4 (2015) 27066. [PubMed: 25979354]

[11]. Rahman M, Ravichandran R, Bansal S, Sanborn K, Bower S, Eschbacher J, Sureshbabu A, Fleming T, Bharat A, Walia R, Hachem R, Bremner RM, Smith MA, Mohanakumar Thalachallour, Novel role for tumor suppressor gene, liver kinase B1, in epithelial-mesenchymal transition leading to chronic lung allograft dysfunction., Am J Transplantation, 00 (2021) 1–10.

[12]. Pain M, Bermudez O, Lacoste P, Royer PJ, Botturi K, Tissot A, Brouard S, Eickelberg O, Magnan A, Tissue remodelling in chronic bronchial diseases: from the epithelial to mesenchymal phenotype, Eur Respir Rev, 23 (2014) 118–130. [PubMed: 24591669]

[13]. Borthwick LA, Parker SM, Brougham KA, Johnson GE, Gorowiec MR, Ward C, Lordan JL, Corris PA, Kirby JA, Fisher AJ, Epithelial to mesenchymal transition (EMT) and airway remodelling after human lung transplantation, Thorax, 64 (2009) 770–777. [PubMed: 19213777]

[14]. Lu YZ, He XL, Liu F, Cheng PP, Liang LM, Wang M, Chen SJ, Huang Y, Yu F, Xin JB, Ye H, Song LJ, Ma WL, Bleomycin induced apical-basal polarity loss in alveolar epithelial cell contributes to experimental pulmonary fibrosis, Exp Cell Res, 396 (2020) 112295. [PubMed: 32971116]

[15]. Verleden SE, Vos R, Vanaudenaerde BM, Verleden GM, Chronic lung allograft dysfunction phenotypes and treatment, Journal of thoracic disease, 9 (2017) 2650–2659. [PubMed: 28932572]

[16]. Li J, Liu J, Li P, Mai X, Li W, Yang J, Liu P, Loss of LKB1 disrupts breast epithelial cellpolarity and promotes breast cancer metastasis and invasion., J Exp Clin Cancer Res, 33(1) (2014) 70. [PubMed: 25178656]

[17]. Shackelford DB, Shaw RJ, The LKB1-AMPK pathway: metabolism and growth control in tumour suppression, Nat Rev Cancer, 9 (2009) 563–575. [PubMed: 19629071]

[18]. Roy BC, Kohno T, Iwakawa R, Moriguchi T, Kiyono T, Morishita K, Sanchez-Cespedes M, Akiyama T, Yokota J, Involvement of LKB1 in epithelial-mesenchymal transition (EMT) of human lung cancer cells, Lung Cancer, 70 (2010) 136–145. [PubMed: 20207041]

[19]. Ji H, Ramsey MR, Hayes DN, Fan C, McNamara K, Kozlowski P, Torrice C, Wu MC, Shimamura T, Perera SA, Liang MC, Cai D, Naumov GN, Bao L, Contreras CM, Li D, Chen L, Krishnamurthy J, Koivunen J, Chirieac LR, Padera RF, Bronson RT, Lindeman NI, Christiani DC, Lin X, Shapiro GI, Janne PA, Johnson BE, Meyerson M, Kwiatkowski DJ, Castrillon DH, Bardeesy N, Sharpless NE, Wong KK, LKB1 modulates lung cancer differentiation and metastasis, Nature, 448 (2007) 807–810. [PubMed: 17676035]

[20]. Asada N, Sanada K, Fukada Y, LKB1 regulates neuronal migration and neuronal differentiation in the developing neocortex through centrosomal positioning, J Neurosci, 27 (2007) 11769–11775. [PubMed: 17959818]

[21]. Shaw RJ, LKB1 and AMP-activated protein kinase control of mTOR signalling and growth, Acta Physiol (Oxf), 196 (2009) 65–80. [PubMed: 19245654]

[22]. Gui YS, Wang L, Tian X, Li X, Ma A, Zhou W, Zeng N, Zhang J, Cai B, Zhang H, Chen JY, Xu KF, mTOR Overactivation and Compromised Autophagy in the Pathogenesis of Pulmonary Fibrosis, PLoS One, 10 (2015) e0138625. [PubMed: 26382847]

[23]. Nakada D, Saunders TL, Morrison SJ, Lkb1 regulates cell cycle and energy metabolism in haematopoietic stem cells, Nature, 468 (2010) 653–658. [PubMed: 21124450]

[24]. Khayati K, Bhatt V, Hu ZS, Fahumy S, Luo X, Guo JY, Autophagy compensates for Lkb1 loss to maintain adult mice homeostasis and survival, Elife, 9 (2020).

[25]. Shan T, Xiong Y, Kuang S, Deletion of Lkb1 in adult mice results in body weight reduction and lethality, Sci Rep, 6 (2016) 36561. [PubMed: 27824128]

[26]. Hemminki A, Markie D, Tomlinson I, Avizienyte E, Roth S, Loukola A, Bignell G, Warren W, Aminoff M, Hoglund P, Jarvinen H, Kristo P, Pelin K, Ridanpaa M, Salovaara R, Toro T, Bodmer W, Olschwang S, Olsen AS, Stratton MR, de la Chapelle A, Aaltonen LA, A serine/threonine kinase gene defective in Peutz-Jeghers syndrome, Nature, 391 (1998) 184–187. [PubMed: 9428765]

[27]. Calles A, Sholl LM, Rodig SJ, Pelton AK, Hornick JL, Butaney M, Lydon C, Dahlberg SE, Oxnard GR, Jackman DM, Janne PA, Immunohistochemical Loss of LKB1 Is a Biomarker for More Aggressive Biology in KRAS-Mutant Lung Adenocarcinoma, Clin Cancer Res, 21 (2015) 2851–2860. [PubMed: 25737507]

[28]. Puffenberger EG, Strauss KA, Ramsey KE, Craig DW, Stephan DA, Robinson DL, Hendrickson CL, Gottlieb S, Ramsay DA, Siu VM, Heuer GG, Crino PB, Morton DH, Polyhydramnios, megalencephaly and symptomatic epilepsy caused by a homozygous 7-kilobase deletion in LYK5, Brain, 130 (2007) 1929–1941. [PubMed: 17522105]

[29]. Zeqiraj E, Filippi BM, Goldie S, Navratilova I, Boudeau J, Deak M, Alessi DR, van Aalten DM, ATP and MO25alpha regulate the conformational state of the STRADalpha pseudokinase and activation of the LKB1 tumour suppressor, PLoS biology, 7 (2009) e1000126. [PubMed: 19513107]

[30]. Baas AF, Boudeau J, Sapkota GP, Smit L, Medema R, Morrice NA, Alessi DR, Clevers HC, Activation of the tumour suppressor kinase LKB1 by the STE20-like pseudokinase STRAD, EMBO J, 22 (2003) 3062–3072. [PubMed: 12805220]

[31]. Dorfman J, Macara IG, STRADalpha regulates LKB1 localization by blocking access to importin-alpha, and by association with Crm1 and exportin-7, Mol Biol Cell, 19 (2008) 1614–1626. [PubMed: 18256292]

[32]. Mimura T, Walker N, Aoki Y, Manning CM, Murdock BJ, Myers JL, Lagstein A, Osterholzer JJ, Lama VN, Local origin of mesenchymal cells in a murine orthotopic lung transplantation model of bronchiolitis obliterans., Am J Pathol, 185(6) (2015) 1564–1574. [PubMed: 25848843]

[33]. Lee H, Zandkarimi F, Zhang Y, Meena JK, Kim J, Zhuang L, Tyagi S, Ma L, Westbrook TF, Steinberg GR, Nakada D, Stockwell BR, Gan B, Energy-stress-mediated AMPK activation inhibits ferroptosis, Nat Cell Biol, 22 (2020) 225–234. [PubMed: 32029897]

[34]. Thery C, Witwer KW, Aikawa E, Alcaraz MJ, Anderson JD, Andriantsitohaina R, Antoniou A, Arab T, Archer F, Atkin-Smith GK, Ayre DC, Bach JM, Bachurski D, Baharvand H, Balaj L, Baldacchino S, Bauer NN, Baxter AA, Bebawy M, Beckham C, Bedina Zavec A, Benmoussa A, Berardi AC, Bergese P, Bielska E, Blenkiron C, Bobis-Wozowicz S, Boilard E, Boireau W, Bongiovanni A, Borras FE, Bosch S, Boulanger CM, Breakefield X, Breglio AM, Brennan MA, Brigstock DR, Brisson A, Broekman ML, Bromberg JF, Bryl-Gorecka P, Buch S, Buck AH, Burger D, Busatto S, Buschmann D, Bussolati B, Buzas EI, Byrd JB, Camussi G, Carter DR, Caruso S, Chamley LW, Chang YT, Chen C, Chen S, Cheng L, Chin AR, Clayton A, Clerici SP, Cocks A, Cocucci E, Coffey RJ, Cordeiro-da-Silva A, Couch Y, Coumans FA, Coyle B, Crescitelli R, Criado MF, D'Souza-Schorey C, Das S, Datta Chaudhuri A, de Candia P, De Santana EF, De Wever O, Del Portillo HA, Demaret T, Deville S, Devitt A, Dhondt B, Di Vizio D, Dieterich LC, Dolo V, Dominguez Rubio AP, Dominici M, Dourado MR, Driedonks TA, Duarte FV, Duncan HM, Eichenberger RM, Ekstrom K, El Andaloussi S, Elie-Caille C, Erdbrugger U, Falcon-Perez JM, Fatima F, Fish JE, Flores-Bellver M, Forsonits A, FreletBarrand A, Fricke F, Fuhrmann G, Gabrielsson S, Gamez-Valero A, Gardiner C, Gartner K, Gaudin R, Gho YS, Giebel B, Gilbert C, Gimona M, Giusti I, Goberdhan DC, Gorgens A, Gorski SM, Greening DW, Gross JC, Gualerzi A, Gupta GN, Gustafson D, Handberg A, Haraszti RA, Harrison P, Hegyesi H, Hendrix A, Hill AF, Hochberg FH, Hoffmann KF, Holder B, Holthofer H, Hosseinkhani B, Hu G, Huang Y, Huber V, Hunt S, Ibrahim AG, Ikezu T, Inal JM, Isin M, Ivanova A, Jackson HK, Jacobsen S, Jay SM, Jayachandran M, Jenster G, Jiang L, Johnson SM, Jones JC, Jong A, Jovanovic-Talisman T, Jung S, Kalluri R, Kano SI, Kaur S, Kawamura Y, Keller ET, Khamari D, Khomyakova E, Khvorova A, Kierulf P, Kim KP, Kislinger T, Klingeborn M, Klinke DJ 2nd, Kornek M, Kosanovic MM, Kovacs AF, Kramer-Albers EM, Krasemann S, Krause M, Kurochkin IV, Kusuma GD, Kuypers S, Laitinen S, Langevin SM, Languino LR, Lannigan J, Lasser C, Laurent LC, Lavieu G, Lazaro-Ibanez E, Le Lay S, Lee MS, Lee YXF, Lemos DS, Lenassi M, Leszczynska A, Li IT, Liao K, Libregts SF, Ligeti E, Lim R, Lim SK, Line A, Linnemannstons K, Llorente A, Lombard CA, Lorenowicz MJ, Lorincz AM, Lotvall J, Lovett J, Lowry MC, Loyer X, Lu Q, Lukomska B, Lunavat TR, Maas SL, Malhi H, Marcilla A, Mariani J, Mariscal J, Martens-Uzunova ES, Martin-Jaular L, Martinez MC, Martins VR, Mathieu M, Mathivanan S, Maugeri M, McGinnis LK, McVey MJ, Meckes DG Jr., Meehan KL, Mertens I, Minciacchi VR, Moller A, Moller Jorgensen M, Morales-Kastresana A, Morhayim J, Mullier F, Muraca M, Musante L, Mussack V, Muth DC, Myburgh KH, Najrana T, Nawaz M, Nazarenko I, Nejsum P, Neri C, Neri T, Nieuwland R, Nimrichter L, Nolan JP, Nolte-'t Hoen EN, Noren Hooten N, O'Driscoll L, O'Grady T, O'Loghlen A, Ochiya T, Olivier M, Ortiz A, Ortiz LA, Osteikoetxea X, Ostergaard O, Ostrowski M, Park J, Pegtel DM, Peinado H, Perut F, Pfaffl MW, Phinney DG, Pieters BC, Pink RC, Pisetsky DS, Pogge von Strandmann E, Polakovicova I, Poon IK, Powell BH, Prada I, Pulliam L, Quesenberry P, Radeghieri A, Raffai RL, Raimondo S, Rak J, Ramirez MI, Raposo G, Rayyan MS, Regev-Rudzki N, Ricklefs FL, Robbins PD, Roberts DD, Rodrigues SC, Rohde E, Rome S, Rouschop KM, Rughetti A, Russell AE, Saa P, Sahoo S, Salas-Huenuleo E, Sanchez C, Saugstad JA, Saul MJ, Schiffelers RM, Schneider R, Schoyen TH,

Scott A, Shahaj E, Sharma S, Shatnyeva O, Shekari F, Shelke GV, Shetty AK, Shiba K, Siljander PR, Silva AM, Skowronek A, Snyder OL 2nd, Soares RP, Sodar BW, Soekmadji C, Sotillo J, Stahl PD, Stoorvogel W, Stott SL, Strasser EF, Swift S, Tahara H, Tewari M, Timms K, Tiwari S, Tixeira R, Tkach M, Toh WS, Tomasini R, Torrecilhas AC, Tosar JP, Toxavidis V, Urbanelli L, Vader P, van Balkom BW, van der Grein SG, Van Deun J, van Herwijnen MJ, Van Keuren-Jensen K, van Niel G, van Royen ME, van Wijnen AJ, Vasconcelos MH, Vechetti IJ Jr., Veit TD, Vella LJ, Velot E, Verweij FJ, Vestad B, Vinas JL, Visnovitz T, Vukman KV, Wahlgren J, Watson DC, Wauben MH, Weaver A, Webber JP, Weber V, Wehman AM, Weiss DJ, Welsh JA, Wendt S, Wheelock AM, Wiener Z, Witte L, Wolfram J, Xagorari A, Xander P, Xu J, Yan X, Yanez-Mo M, Yin H, Yuana Y, Zappulli V, Zarubova J, Zekas V, Zhang JY, Zhao Z, Zheng L, Zheutlin AR, Zickler AM, Zimmermann P, Zivkovic AM, Zocco D, Zuba-Surma EK, Minimal information for studies of extracellular vesicles 2018 (MISEV2018): a position statement of the International Society for Extracellular Vesicles and update of the MISEV2014 guidelines, J Extracell Vesicles, 7 (2018) 1535750. [PubMed: 30637094]

[35]. Zeqiraj E, Filippi BM, Deak M, Alessi DR, van Aalten DM, Structure of the LKB1-STRAD-MO25 complex reveals an allosteric mechanism of kinase activation, Science, 326 (2009) 1707–1711. [PubMed: 19892943]

[36]. Nedaeinia R, Manian M, Jazayeri MH, Ranjbar M, Salehi R, Sharifi M, Mohaghegh F, Goli M, Jahednia SH, Avan A, Ghayour-Mobarhan M, Circulating exosomes and exosomal microRNAs as biomarkers in gastrointestinal cancer, Cancer Gene Ther, 24 (2017) 48–56. [PubMed: 27982021]

[37]. Liu Q, Piao H, Wang Y, Zheng D, Wang W, Circulating exosomes in cardiovascular disease: Novel carriers of biological information, Biomed Pharmacother, 135 (2021) 111148. [PubMed: 33412387]

[38]. Liu W, Bai X, Zhang A, Huang J, Xu S, Zhang J, Role of Exosomes in Central Nervous System Diseases, Front Mol Neurosci, 12 (2019) 240. [PubMed: 31636538]

[39]. Barberis E, Vanella VV, Falasca M, Caneapero V, Cappellano G, Raineri D, Ghirimoldi M, De Giorgis V, Puricelli C, Vaschetto R, Sainaghi PP, Bruno S, Sica A, Dianzani U, Rolla R, Chiocchetti A, Cantaluppi V, Baldanzi G, Marengo E, Manfredi M, Circulating Exosomes Are Strongly Involved in SARS-CoV-2 Infection, Front Mol Biosci, 8 (2021) 632290. [PubMed: 33693030]

[40]. Gunasekaran M, Sharma M, Hachem R, Bremner R, Smith MA, Mohanakumar T, Circulating Exosomes with Distinct Properties during Chronic Lung Allograft Rejection, J Immunol, 200 (2018) 2535–2541. [PubMed: 29491008]

[41]. Sharma M, Gunasekaran M, Ravichandran R, Fisher CE, Limaye AP, Hu C, McDyer J, Kaza V, Bharat A, Tokman S, Omar A, Arjuna A, Walia R, Bremner RM, Smith MA, Hachem RR, Mohanakumar T, Circulating exosomes with lung self-antigens as a biomarker for chronic lung allograft dysfunction: A retrospective analysis, J Heart Lung Transplant, (2020).

[42]. Glanville AR, Verleden GM, Todd JL, Benden C, Calabrese F, Gottlieb J, Hachem RR, Levine D, Meloni F, Palmer SM, Roman A, Sato M, Singer LG, Tokman S, Verleden SE, von der Thusen J, Vos R, Snell G, Chronic lung allograft dysfunction: Definition and update of restrictive allograft syndrome-A consensus report from the Pulmonary Council of the ISHLT, J Heart and Lung Transplantation, 38(5) (2019) 483–492.

[43]. Okon IS, Coughlan KA, Zhang C, Moriasi C, Ding Y, Song P, Zhang W, Li G, Zou MH, Protein kinase LKB1 promotes RAB7-mediated neuropilin-1 degradation to inhibit angiogenesis, J Clin Invest, 124 (2014) 4590–4602. [PubMed: 25180605]

[44]. Igarashi N, Honjo M, Aihara M, mTOR inhibitors potentially reduce TGF-beta-2induced fibrogenic changes in trabecular meshwork cells, Sci Rep, 11 (2021) 14111. [PubMed: 34239027]

[45]. Kim J, Kundu M, Viollet B, Guan KL, AMPK and mTOR regulate autophagy through direct phosphorylation of Ulk1, Nat Cell Biol, 13 (2011) 132–141. [PubMed: 21258367]

[46]. Liu S, Zhang J, Yu B, Huang L, Dai B, Liu J, Tang J, The role of autophagy in lung ischemia/reperfusion injury after lung transplantation in rats, Am J Transl Res, 8 (2016) 3593–3602. [PubMed: 27648150]

Highlights

- Increased levels of circulating exosomes by days 14 and 34 after murine lung transplantation
- LKB1 expression is downregulated in circulating exosomes in transplanted mice.
- LKB1 expression is downregulated in donor lung tissue in transplanted mice.
- LKB1, STRADα, and pAMPK were downregulated, but phosphorylated mTOR was upregulated in donor lungs.
- Histological evidence of chronic rejection in the transplanted but not native lung.

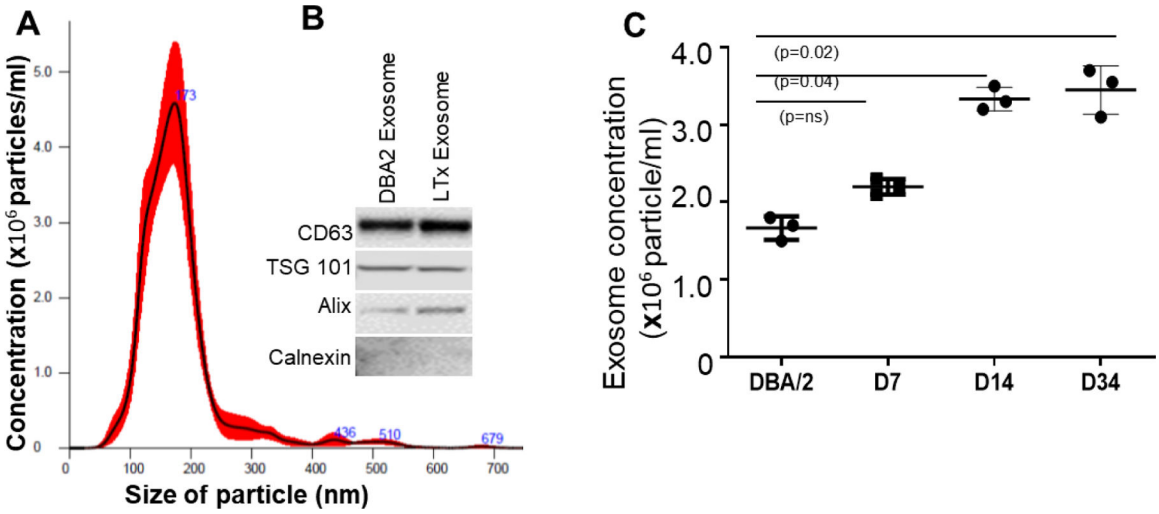

Figure 1:

Characterization of exosomes derived from mouse serum by nanoparticle tracking analysis. (A) According to the size, the particles are considered as exosomes (40–200 nm). (B) The exosome expressed CD63, TSG 101, and Alix but not Calnexin. (C) Exosome particle/ml are significantly higher in day-14 (n=3, p=0.04), day-34 (n=3, p=0.02) serum compared to non-transplanted DBA/2 serum. Values are mean ± SD; all values represent at least three independent experiments.

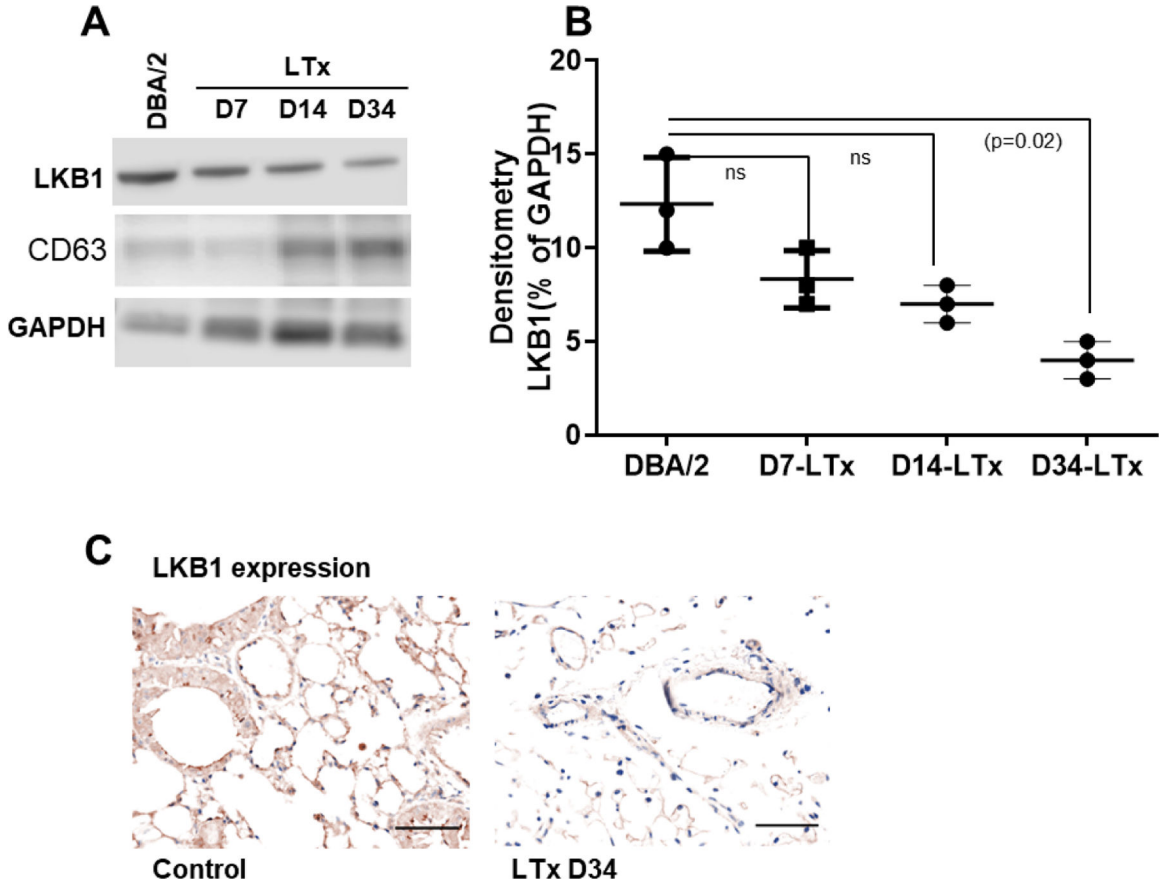

Figure 2:

LKB1 expression in mouse exosome and donor lung tissue. (A) Western blot analysis of LKB1 in exosomal protein isolated from transplanted (day-7, -14, and -34). Control exosome was isolated from non-transplanted DBA/2 mice. CD63 was used as exosome marker, and GAPDH was used as internal loading control. (B) Densitometry analysis showed significant downregulation of LKB1 expression in exosomal protein derived from day-7, -14, and -34 (n=3, p=0.02) after LTx compared to non-transplanted DBA/2 mice. (C) Representative Immunohistochemistry picture of LKB1 expression in donor and recipient lung tissue at day 34 after transplantation. The scale bar is 40x magnification and dimension is 50μm.

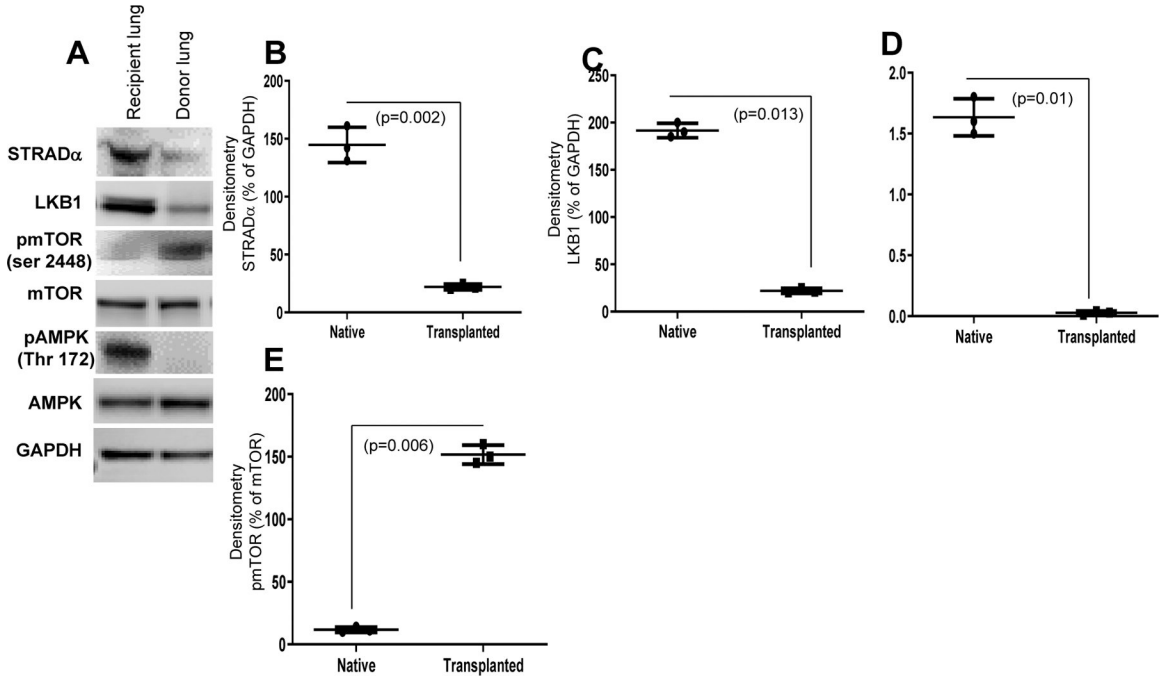

Figure 3:

(**A**) LKB1 expression is downregulated in donor lungs compared to recipient lungs at day 34. Representative immunohistochemistry of LKB1 expression in donor and recipient lung tissue at day 34 after LTx. (**B**) STE20-related adaptor alpha (STRADα, LKB1, pAMPK expression is downregulated and pmTOR expression is upregulated in donor lungs compared to recipient lungs at day 34, as detected by western blot analysis. (**C, D, E, F**) Densitometry analysis showed significant downregulation of STRADα (n=3, p=0.002), LKB1 (n=3, p=0.013), and pAMPK (n=3, p=0.01) and upregulation of pmTOR (n=3, p=0.006). Values are mean ± SD of three independent experiments. Abbreviations: AMPK, AMP-activated protein kinase; mTOR, mammalian target of rapamycin.

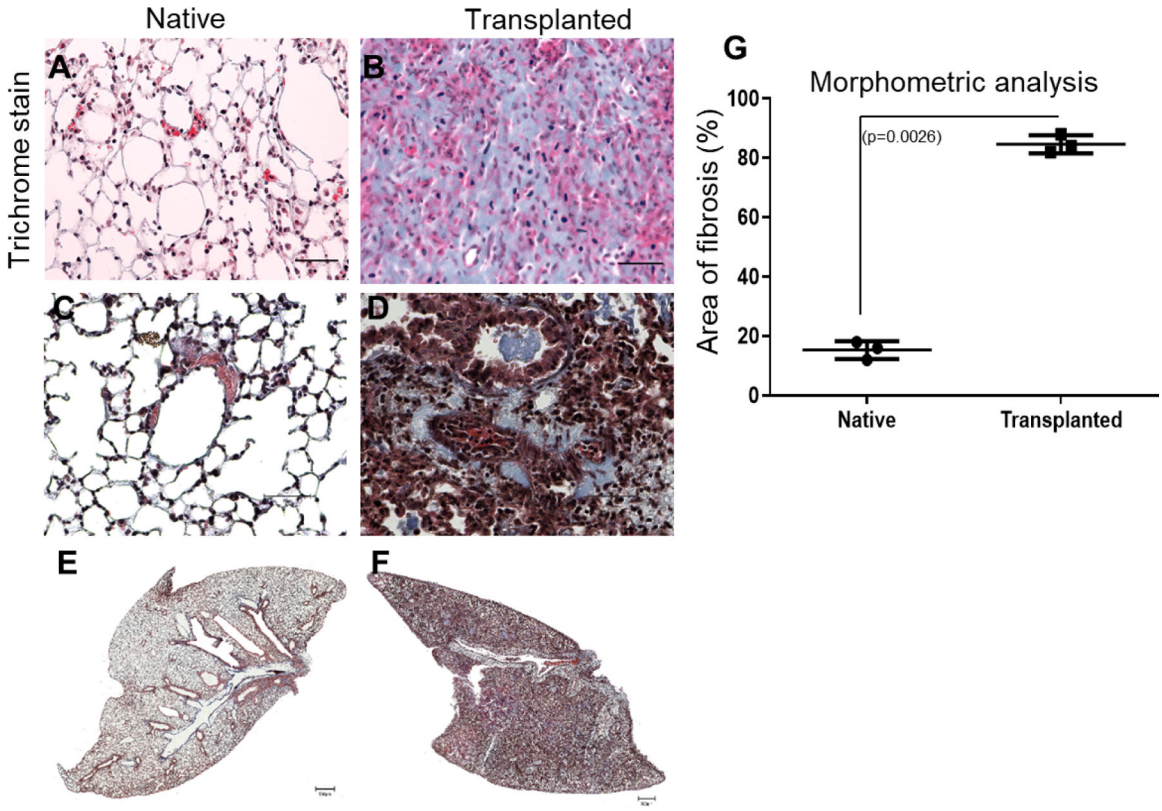

Figure 4:

Histological lesions consistent with chronic rejection and the development of fibrosis in a B6D2F1 to DBA/2 orthotopic LTx murine model as detected by immunohistochemistry. Cut sections were stained with Masson's trichrome to determine the presence of fibrosis. Masson's trichrome (**A, B**) staining in native and transplanted lung tissue. Morphometric analysis of fibrosis: Areas of interest were manually demarcated and measured as a fraction of the total tissue area using ImageJ software (**C**). Histopathological studies with native lung with normal bronchioles and (D) after murine lung transplantation with perivascular and peri-bronchial fibrosis along with fibrotic plugs. (The scale bar is 40x magnification and dimension is 50μm). Representative Whole lobe scanned image of masson trichrome staining using Invitrogen EVOS M7000 for (E) Native lung (F) Transplanted lung. (The scale bar is 500μm) (n=3).

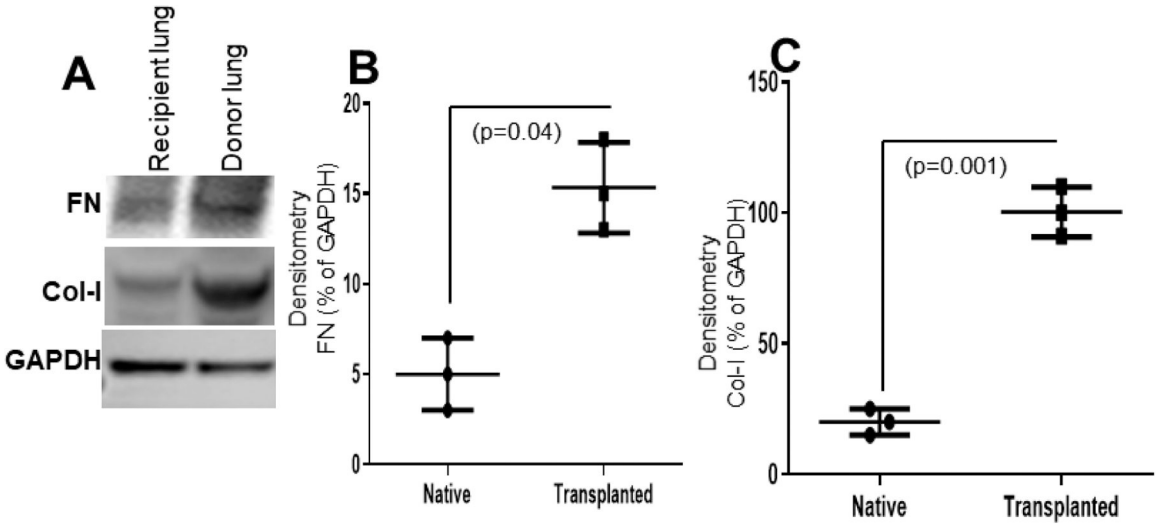

Figure 5:

FN and Col-I, both markers of fibrosis, in donor and native recipient lungs. (**A**) FN and Col-I were upregulated in donor lungs compared to native recipient lungs as shown by western blot analysis. (**B, C**) Densitometry analysis showed significant upregulation of FN (n=3, p=0.04) and Col-I (n=3, p=0.001) in donor lungs. Values are mean ± SD of three independent experiments.

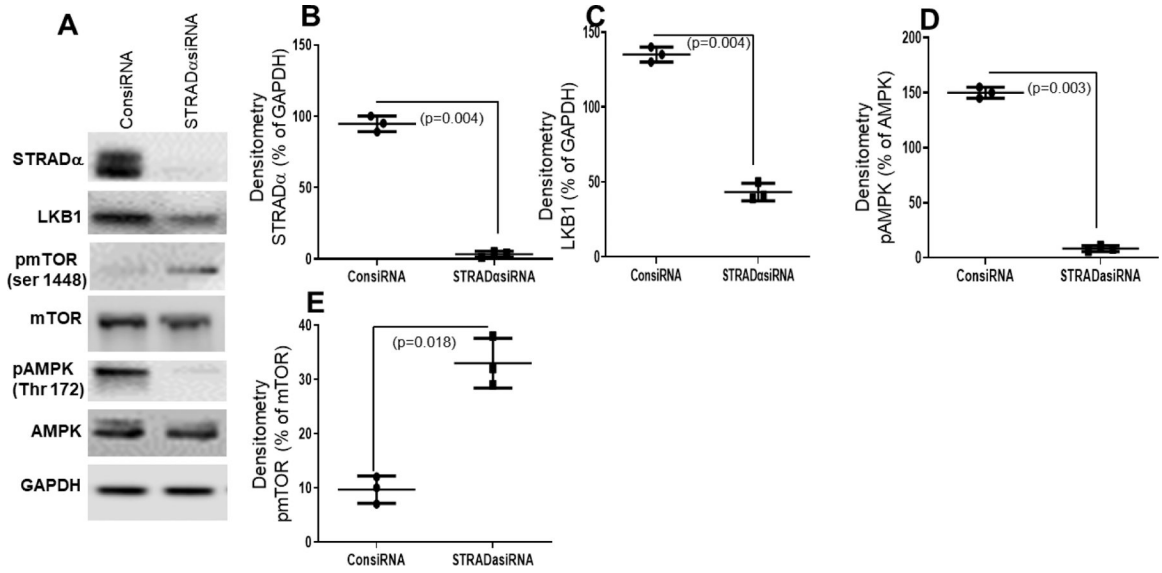

Figure 6:

Effect of STRADα knockdown by siRNA on BEAS-2B cells. (**A**) Western blot analysis of STRADα, LKB1, and pAMPK expression in BEAS-2B cells after STRADα knockdown by siRNA (STRADα siRNA) or knockdown with control (ConsiRNA). (**B, C, D, E**) Densitometry analysis showed knockdown of STRADα by siRNA significantly downregulated LKB1 (n=3, p=0.004) and pAMPK (n=3, p=0.003) and upregulated pmTOR (n=3, p=0.018). Values are mean ± SD of three independent experiments.

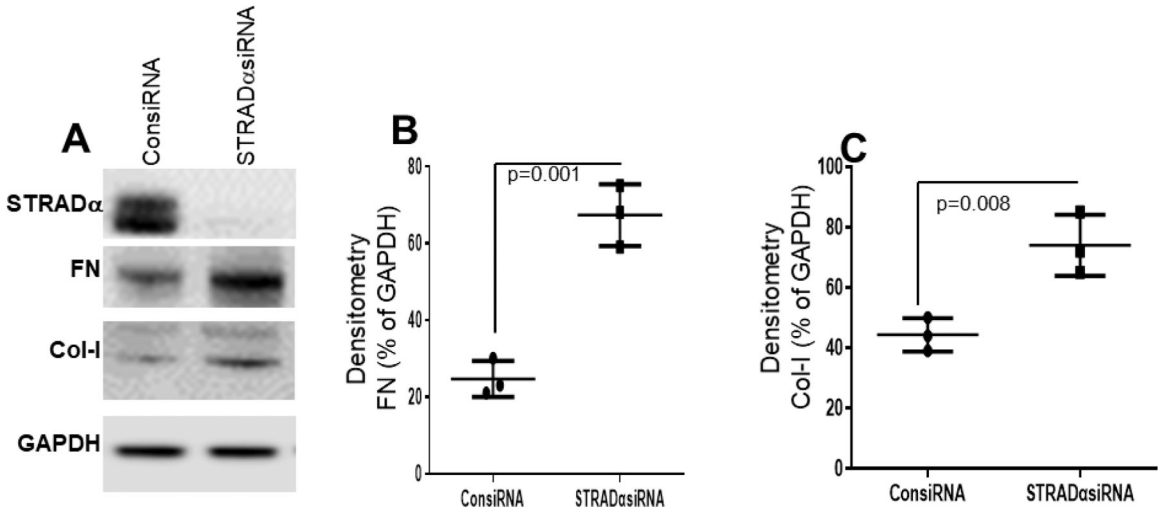

Figure 7:

STRADα knockdown by siRNA significantly upregulated fibrosis markers (FN and Col-I) in BEAS-2B cells. (**A**) Western blot analysis of STRADα, FN, and Col-I expression in BEAS-2B cells after STRADα knockdown by siRNA (STRADα siRNA) or knockdown with control (ConsiRNA). (**B, C**) Densitometry analysis showed knockdown of STRADα significantly upregulated FN (n=3, p=0.001) and Col-I (n=3, p=0.008). Values are mean ± SD of three independent experiments.

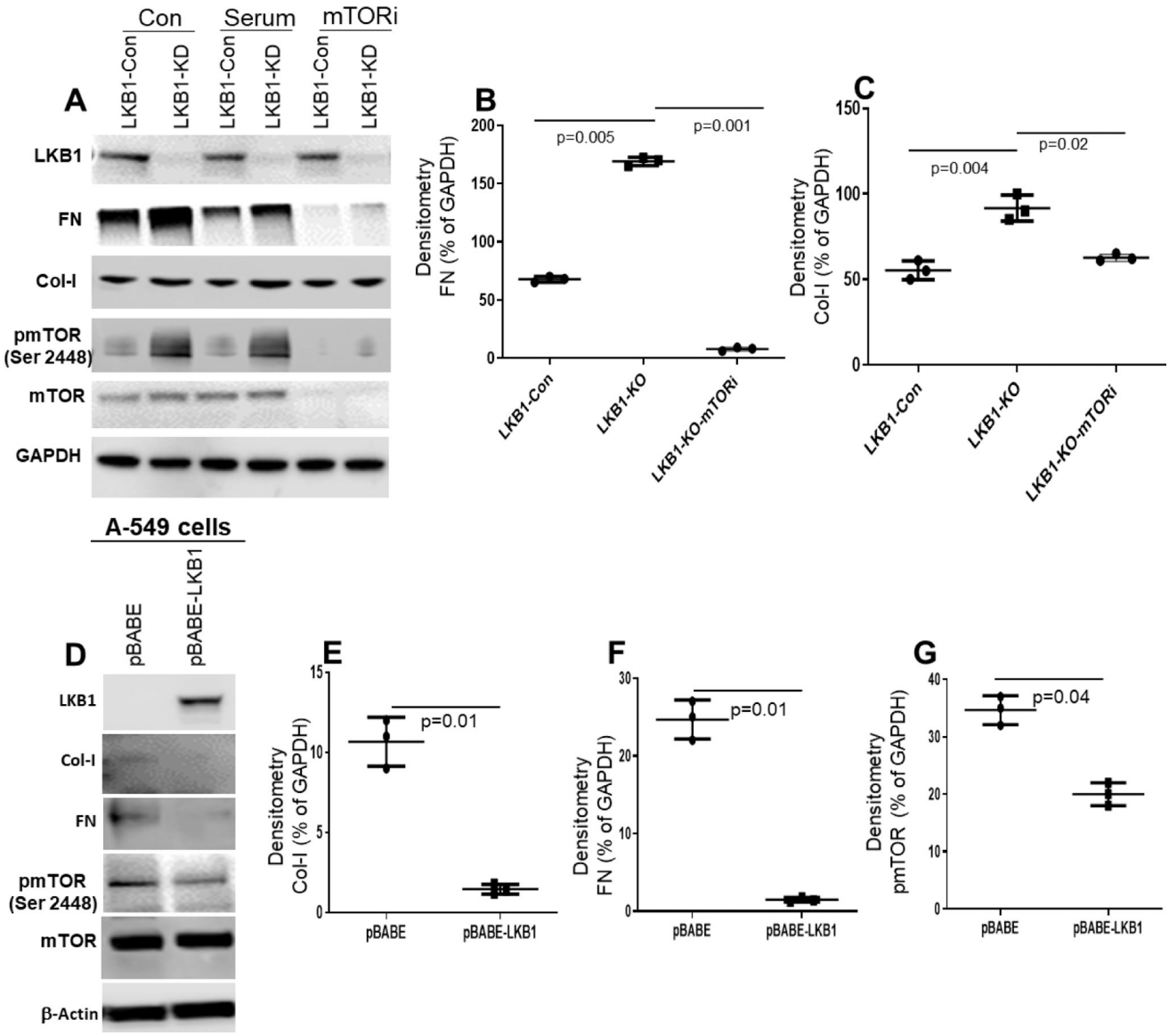

Figure 8:

Effect of mTOR inhibitor on control and LKB1 knockdown BEAS-2B cells. (**A**) Western blot analysis of LKB1, FN, Col-I, and pmTOR expression in control and LKB1 knockout BEAS-2B cells after treatment with mTOR inhibitor. (**B, C**) Densitometry analysis showed FN (n=3, p=0.001) and Col-I (n=3, p=0.02) expression are significantly downregulated in LKB1 knockout BEAS-2B cells treated with mTOR inhibitor (mTORi) compared to control cells. (**D**) Overexpression of LKB1 downregulates FN, Col-I, and pmTOR in A549 cells. (**E, F, G**) Densitometry analysis showed Col-I (n=3, p=0.01), FN (n=3, p=0.01), and pmTOR (n=3, p=0.04) expression are significantly downregulated in pBABE-LKB1 compared to pBABE. Values are mean ± SD of three independent experiments.

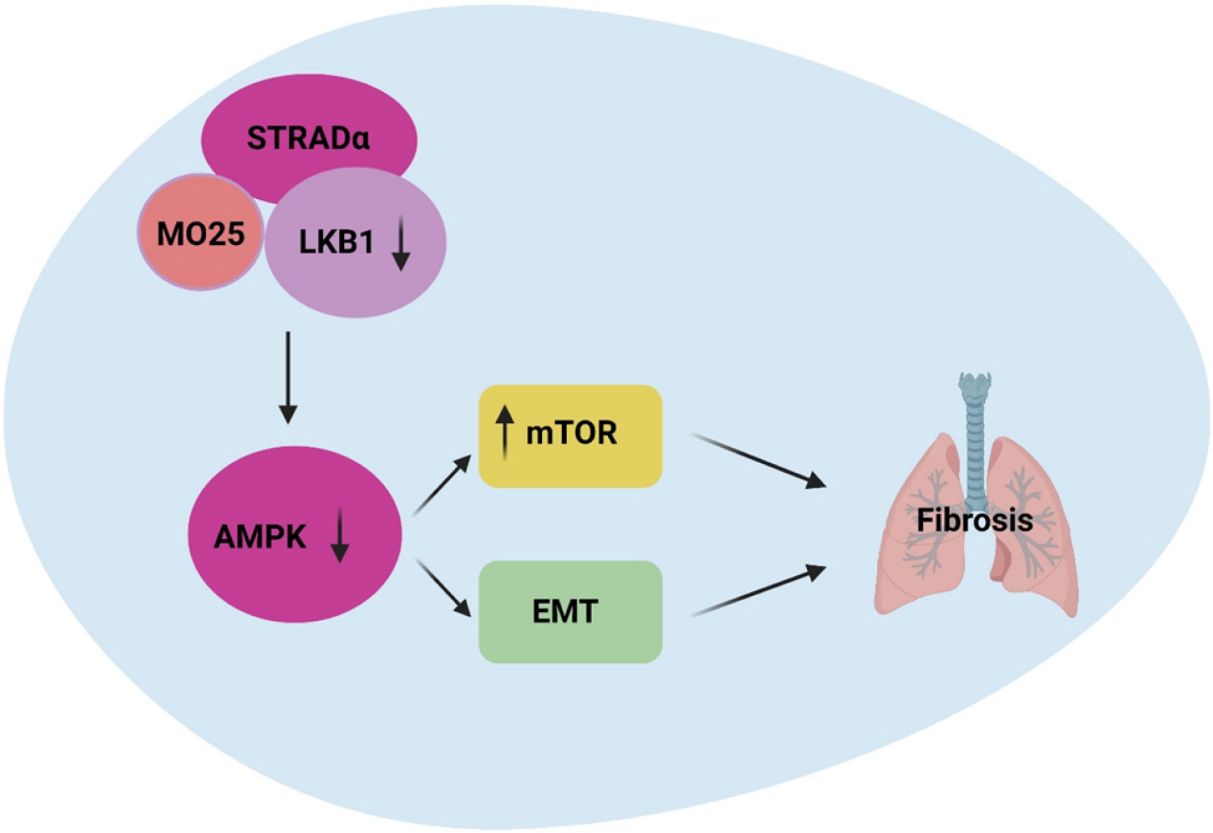

Figure 9:

Schematic diagram of LKB1 deficiency and development of lung fibrosis via AMPK and mTOR induction. Master kinase LKB1 signaling pathways, complexed with its two regulatory subunits STRADα and MO25, phosphorylates and activates AMPK. In turn, these kinases induce phosphorylate of mTOR and induce EMT playing important role in the pathogenesis of fibrosis after LTx.